https://dx.doi.org/10.21577/0103-5053.20210113

J. Braz. Chem. Soc., Vol. 32, No. 12, 2215-2221, 2021

Article

Arrays of Copper Microelectrodes from Disposable Chips: Fabrication and Characterization

Giane S. Higino,[a] Ítalo R. Machado,[b] Gabriel F. Nascimento[c] and Jairo J. Pedrotti[*,c]*

[a]*Centro de Pesquisas Avançadas em Grafeno e Nanomateriais, MackGraphe, 01302-907 São Paulo-SP, Brazil*

[b]*Instituto de Química, Universidade de São Paulo, 05513-907 São Paulo-SP, Brazil*

[c]*Escola de Engenharia, Universidade Presbiteriana Mackenzie, 01302-907 São Paulo-SP, Brazil*

A simple, fast, and low-cost process to fabricate arrays of copper microelectrodes (CuMEs) based on disposable electronic microchips is described. Arrays with 8 to 20 CuMEs were characterized by energy-dispersive X-ray spectroscopy and cyclic voltammetry techniques. The closest interelectrode distance in the arrays is 358 ± 22 μm, and the minor radius ranged from 10.6 to 13.5 μm. The microchips with CuMEs were sealed in epoxy resin to fabricate the rod and flat-shaped platforms, allowing the CuMEs to be addressed separately. Glucose, hydrazine, and nitrate were used as analyte models for voltammetric and amperometric detection at CuMEs arrays, showing excellent performance in batch and flow-through cells. Glucose measurements carried out with flow injection analysis system with amperometric detection at an array of 20 CuMEs showed a wide linear range (0.020-4.0 mmol L^{-1}), high sensitivity (734.1 μA L $mmol^{-1}$ cm^{-2}), and a limit of detection of 1.7 μmol L^{-1}.

Keywords: copper microelectrode arrays, glucose, nitrate, electrochemical detection, flow analysis

Introduction

Copper electrodes have attractive use as electrochemical due to their low cost, good mechanical stability, high electrical conductivity, and easy use in microfabrication processes.[1,2] Additionally, depending on solution composition, the copper surface can also be quickly renewed by electrochemical treatment during the measurements steps to minimize its passivation due to its side-reactions with the sample or electrolyte components.[3,4] Macro and micro-copper electrodes of different shapes have been investigated for applications in environmental, industrial, clinical, and pharmaceutical fields.[5-9] On the other hand, the use of microelectrodes offers significant advantages over large-size electrodes, including the radial diffusion dominance, which yields a sigmoid voltammetric curve, and a reduced capacitive charging current that allows improving the sensitivity of electroanalytical sensors. They can also provide fast cell-response time and negligible ohmic potential drop (iR drop) in the electrochemical cell, facilitating the operation by a simple two-electrode system.

*e-mail: jpedrotti@mackenzie.br

Further, the electrodes with ultrasmall dimensions are compatible with monitoring chemical species in microenvironments, stimulating applications in different science fields.[10-13] However, one disadvantage associated with ultramicroelectrode is the low faradaic current signal (usually at nA or pA levels) generated during the electrochemical process when a single sensor is used. In order to mitigate this drawback, the use of microelectrode arrays is recommended since each microelectrode working in parallel can individually contribute to the total measured current. Microelectrodes arrays can also assure the detector response even when some microelectrode is not active, which does not happen when only a single microelectrode is used.

Different techniques have been used to prepare copper microelectrodes arrays, including photolithography, electrodeposition, and Cu flat flexible cables.[2,14-16] Among these techniques, the photolithography processes are more common. They allow the fabrication of a large number of microelectrodes easily controlled and highly reproducible in size. However, these processes usually demand clean-room, high-cost instrumentation, and highly qualified operators.

In this work, a low-cost and straightforward process to fabricate platforms of copper microelectrodes arrays with 8 to 20 units obtained from microchips is described. The new microsensor arrays were characterized by energy-dispersive X-ray spectroscopy and cyclic voltammetry techniques. The copper microelectrodes (CuMEs) platforms were evaluated for glucose, hydrazine, and nitrate electrochemical measurements in batch and flow-through cells, showing excellent performance.

Experimental

Reagents and solutions

All reagents were analytically graded and were used without further purification. The stock solutions and subsequent dilutions were prepared by using deionized water with a resistivity of 18.2 MΩ cm obtained from the Smart Park Millipore (Merck, Darmstadt, Germany) purification system. The analytical solutions were prepared daily just before their use. The epoxy resin and the catalyst used for polymer curing were purchased at Redelease Co. (São Paulo, Brazil).

Preparation of CuMEs platforms

The copper microelectrodes were prepared from surface mounted device (SMD) disposable microchips provided with 8 to 20 pins, which use copper microwires to connect the active part of the integrated circuit to the external terminals of a semiconductor. The code and the manufacturer of the SMD components often used to fabricate the CuMEs are in Supplementary Information (SI) section.

The copper microdisks manufacture starts with the upper polymeric part of the chip removal with a help of a sandpaper of 800 mesh, which is followed until the complete disruption of the copper wires bonding, according to the procedure previously described.[17] Afterward, the copper disks are carefully polished with sandpapers ranging from 1,000 to 3,000 mesh until they reach disks with a well-defined elliptical shape. This step is followed by visual inspections in an optical microscope at the end of each stage. In the last step, the Cu microdisks are polished with alumina with 0.50 and 0.03 μm granulometry, followed by a short cleanness step by rinsing with deionized water. The chip is transferred to a beaker with deionized water at the next step, and it was sonicated for 10 min. This cleaning process was repeated at least five times for residues removal remained after the polishing process. Figure 1a shows a typical SMD microchip used to fabricate the CuMEs, the distribution of the CuMEs on the array (Figure 1b), and the usual shape of a random CuME (Figure 1c).

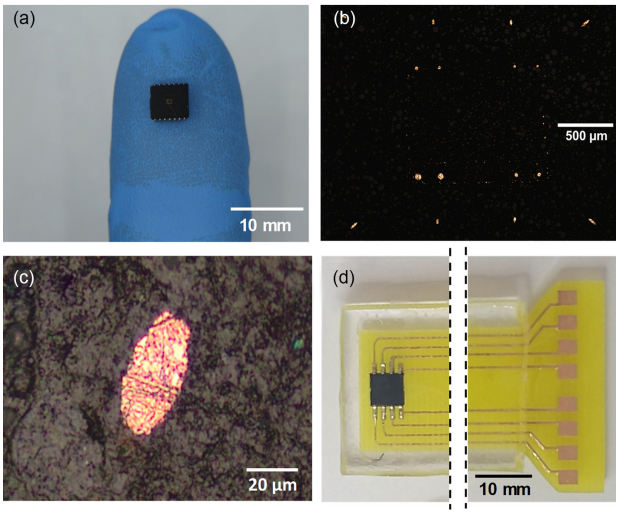

Figure 1. Image of a microchip with 14 pins (a); optical image of an array of eight microelectrodes (b); one single and random copper microelectrode (c); flat platform (d).

The chip with Cu microdisks was then fixed with Pb-Sn solder on a printed circuit board (20 × 50 mm) to ensure an independent electrical contact with each microdisk. Next, the chip was pressed on a double-faced adhesive tape, previously glued on a 10 × 10 mm glass plate. Afterward, a polyethylene mold (40 mm long × 2 mm high × 25 mm wide) was placed on the adhesive tape. The glass surface was then vertically positioned on the bench with the help of a clamp connected to a lab support stand to fill the mold with epoxy resin. The flat platform obtained after the resin curing process for around 6 h is depicted in Figure 1d.

Thin wires were welded, for platform fabrication in rod-shaped, at the external terminals of the microchip to make the individual electric contact with the copper disks.

Afterward, the polished chip was positioned at the tip of a high-density polyethylene tube (inner diameter (i.d.) = 10 mm), carefully filled with epoxy resin serving as the mold.

Before its use, the CuMEs have rinsed with acetone for removing any glue residues from the adhesive tape used to fix the chip inside the mold. In routine use, the surface of the microelectrodes was cleaned with alumina mechanical polishing. However, after some days without using the copper electrodes, sometimes was observed a dark layer covering partially or totally their surface, suggesting the copper oxide formation. So, in this condition, just alumina mechanical polishing was not enough to properly cleaning the electrodes. As for this condition, we used a 0.10 mol L^{-1} HCl solution drop in contact with the microdisks for a short period, no more than 60 s, followed by a rinse with

deionized (DI) water. The visual effect of this chemical treatment can be seen in Figure S1, SI section.

Flow cell design

The flow cell consists of two acrylic blocks (40 mm wide, 10 mm high, and 40 mm long) affixed by four brass screws. A schematic diagram of the flow cell built in the laboratory is depicted in Figure 2. A central hole (8.0 × 5.0 mm) was made in the upper block (Figure 2b) with an internal volume of 1.0 mL, to insert the three electrodes, the inlet, and the outlet solution. A polyetheretherketone (PEEK) tubing 30 mm long (i.d. = 0.3 mm) was used to conduct the solution onto the CuMEs array working electrode. The Ag/AgCl reference electrode (3.0 mol L^{-1} KCl),[18] was positioned beside the PEEK tubing. A stainless-steel tubing (i.d. = 1.5 mm) was utilized as the auxiliary electrode and outlet solution. The O-ring of Viton® inserted between the two acrylic blocks helped to adapt the working electrode in the electrochemical cell, avoiding electrolyte leakage.

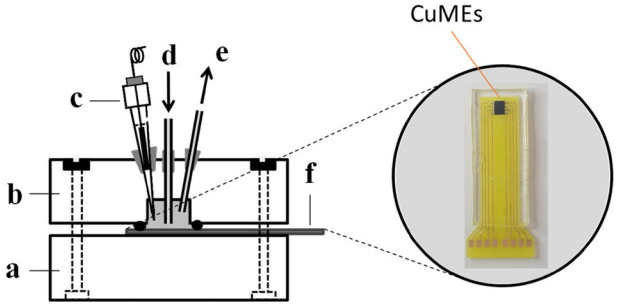

Figure 2. Schematic diagram of the wall-jet flow-through cell; (a) and (b) acrylic blocks; (c) Ag/AgCl reference electrode; (d) inlet solution; (e) auxiliary electrode and outlet solution; (f) CuMEs working electrode. In detail, a platform with an array of CuMEs working electrode.

Instrumentation

The CuMEs fabrication was followed by visual inspection by using a microscope Olympus model X51M (Nagano, Japan) provided with magnification lenses from 10 to 100 times. The energy X-ray dispersive spectroscopy (EDS) analyses were performed with a scanning electron microscopy JEOL, model JSM-7800F (Tokyo, Japan), by using an acceleration voltage of 10 KeV. The electrochemical measurements were carried out by using a μAutolab potentiostat computer-controlled by NOVA V.1.1 (Herisau, Switzerland) software combined with a lab-made Faraday cage to protect the electrochemical cell from the interference of environmental noise. The cyclic voltammetry measurements were performed with a conventional electrochemical cell (10 mL internal volume) using CuMEs as a working electrode, an Ag/AgCl reference electrode, and a Pt wire as the auxiliary electrode. The flow cell described in "Flow cell design" sub-section was used for glucose amperometric detection in the flow injection system. The solutions were propelled with an Ismatec peristaltic pump, MS-REGLO model (Glattbrugg, Switzerland). Samples and analytical solutions were injected into the flow injection analysis (FIA) system with a homemade, manually operated rotatory valve provided with a 100 μL loop volume. All measurements were performed at 22 ± 1.0 ºC temperature.

Results and Discussion

The CuMEs fabrication process is simple, cheap, and requires neither special tools nor a highly skilled operator. The Cu microelectrodes are usually ellipse-shaped (Figure 1c) and arranged in an almost circular pattern on the chip surface. The CuMEs show a minor radius of 12.4; 10.6 and 13.5 μm in arrays of 8, 14, and 20 microelectrodes, respectively, and the mean center-to-center distance between the two closest electrodes higher than 370 μm, which is more than 27 times higher than the radius in the most density packaged array. This information suggests little or no overlap of diffusion layers between the electrodes in the array. At this condition, the measured current signal is amplified by the number of active electrodes contained in the array.[19] Table S1 (SI section) shows additional geometric information of the proposed CuMEs arrays. Figure S2 (SI section) shows the contribution of each Cu microelectrode in an array with eight microelectrodes. As can be seen, the sum of the limiting current of each electrode represents more than 99% of the limiting current of the array (Figure S2f), evidencing the advantage of using the CuMEs array for electroanalytical applications.

Characterization of microelectrodes

Energy-dispersive X-ray measurements were performed to evaluate the chemical composition of the microdisks. A typical EDS spectrum of a microdisk sample obtained from an array containing 20 units is shown in Figure 3a. The elemental composition consisted mainly of Cu and small amounts of carbon and aluminum in the samples. According to the EDS results, the atomic proportions are 93.7% copper, 5.5% carbon, and 0.8% aluminum. The voltammetric profile of a CuMEs array with eight units in a 0.50 mol L^{-1} NaOH solution was examined in the potential window of −1.5 to 0.80 V *vs*. Ag/AgCl at a scan rate of 25 mV s^{-1}. The peak signals in Figure 3b can be attributed to various oxidation states of copper in alkaline solution, according to previous studies[20-22] carried

out with metallic copper electrodes in alkaline solution. The first anodic current peak at –0.39 V (A_I) corresponds to the oxidation of metallic copper to its first oxidation state, Cu^I. The second anodic signal peak at –0.07 V(A_{II}) is assigned to Cu^{II} formation, resulting of oxidative processes of Cu^0/Cu^{II} and Cu^I/Cu^{II}.[20,21] The different electrochemical processes between 0.40 and 0.80 V lead to peak distortion, as the shoulder is close to 0.18 V.[21,22] The third and discrete peak anodic observed at 0.52 V (A_{III}) is frequently described by the presence of Cu^{III} that appears in the form of CuOOH or $Cu(OH)_4^-$.[22-25] The species of Cu^{III} are unstable and highly oxidizing, being attractive to some electrocatalytic oxidation processes, particularly for analytical applications.[26-28]

At the reverse scan rate, the I-E curve presents two characteristic cathodic peaks at –0.56 and –0.92 V, corresponding to the regeneration of Cu^I and Cu^0, respectively.[22,29,30] Thus, in general, our finds with the proposed CuMEs suitably fit the previous studies[20-25,29,30] carried out with copper electrodes in alkaline solutions.

Analytical performance

To evaluate the analytical performance of the CuMEs, we used glucose and hydrazine as the analyte models for preliminary voltammetric measurements. Figure 4A shows the typical voltammetric response for glucose at 2.0 to 9.5 mmol L^{-1} concentration range at eight CuMEs in 0.10 mol L^{-1} NaOH solution by sweeping the potential between –0.20 to +0.65 V at a scan rate of 20 mV s^{-1}. At the electrolyte solution, the CV showed a low residual current at window potential from –0.20 to +0.65 V. At solutions containing glucose, the anodic current signals presented well-defined sigmoidal waves, indicating that the spherical diffusion corresponded to the analyte dominance process toward the CuOMEs surface.

The voltammetric CuOMEs response for hydrazine at 200-570 µmol L^{-1} concentration range in alkaline solution is depicted in Figure 4B. The well-defined voltammetric waves confirm the excellent performance of the CuOMEs for N_2H_4 sensing.

The anodic current from N_2H_4 oxidation to N_2 started at +0.023 V and reached the limiting-current region at around +0.40 V, and extended up to +0.60 V. The anodic steady-state current signals rose linearly with the increasing concentrations for both electroactive species, as it can be seen in the insets, and obeyed the following equations: I (nA) = –3.96 + 49.6 × $C_{glucose}$, mmol L^{-1} and I (nA) = –0.406 + 86.5 × $C_{hydrazine}$, µmmol L^{-1}.

Nitrate has a great interest in the environmental field,

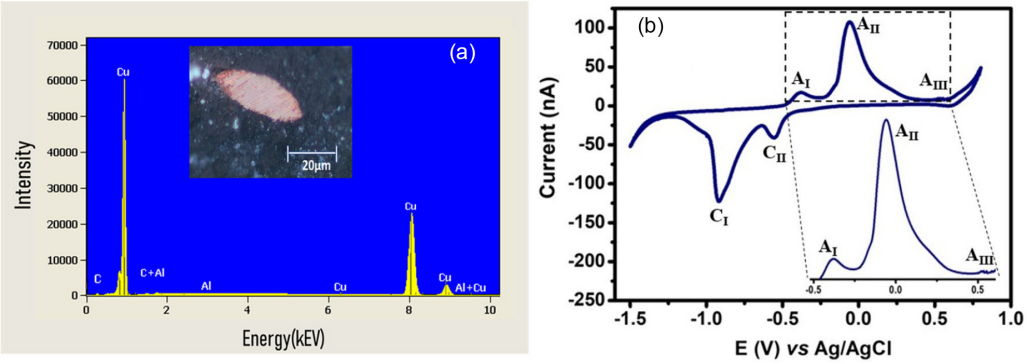

Figure 3. Energy dispersive X-ray elemental analysis of a CuME (a) and a typical cyclic voltammogram obtained with eight CuMEs in 0.5 mol L^{-1} NaOH at 25 mV s^{-1} scan rate (b).

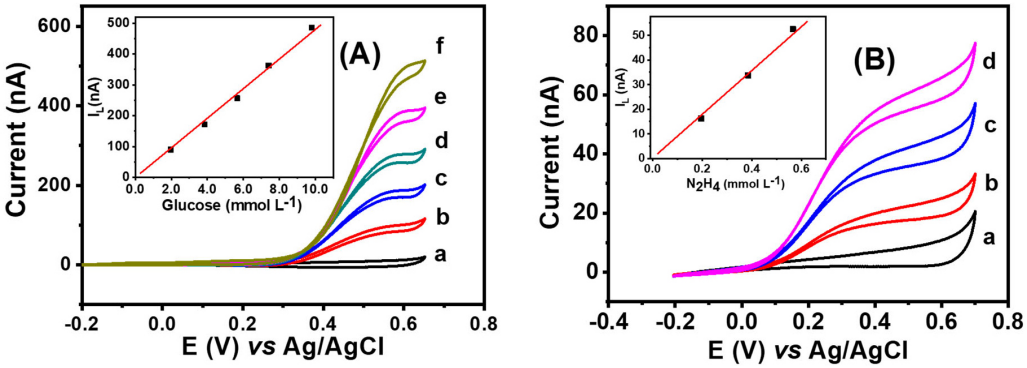

Figure 4. Voltammetric glucose response (A) and N_2H_4 (B) on an array of CuMEs in 0.10 mol L^{-1} NaOH. Glucose concentration: (a) 0.0; (b) 2.0; (c) 3.8; (d) 5.7; (e) 7.4; (f) 9.5 mmol L^{-1}. N_2H_4 concentration: (a) 0.0; (b) 200; (c) 390; (d) 570 µmol L^{-1}. Scan rate: 20 mV s^{-1}.

and it is electroactive at copper electrode surfaces in acidic media through a reduction step involving an eight-electron transfer (equation 1). Depending on the supporting electrolyte composition, this step can occur from –0.45 to –0.70 V *versus* saturated calomel electrode (SCE).[31]

$$NO_3^- + 8e^- + 10H^+ \rightleftarrows NH_4^+ + 3H_2O \quad (1)$$

We used a platform with twenty CuMEs to evaluate the square wave voltammetry response for nitrate detection at 75-440 μmol L^{-1} concentration range in 0.10 mol L^{-1} Na_2SO_4 + 0.050 mol L^{-1} KCl electrolyte solution at pH 2.0. The square wave voltammograms obtained showed well-shaped cathodic peaks resulting from nitrate reduction that started at –0.39 V and attained a maximum at –0.53 V, as shown in Figure 5. An analysis of the current peak signals *versus* nitrate concentration (inset) by linear regression showed an R-square = 0.998 and obeyed the equation: I (nA) = $-1.94 - 0.22 \times C_{nitrate}$. At this condition, the limit of detection (3 × standard deviation of the blank response ($3\sigma_{blank}$)) was estimated at 17.8 μmol L^{-1} and the limit of quantification at 53.3 μmol L^{-1}, suggesting that the proposed CuMEs platforms can be a good analytical tool for nitrate determination in drinking and natural waters.[4,32]

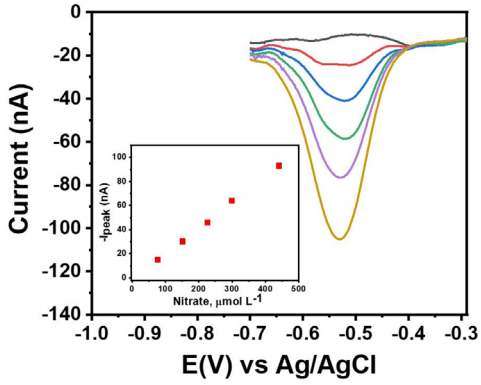

Figure 5. Square wave voltammograms of nitrate at an array of twenty CuMEs in 0.10 mol L^{-1} Na_2SO_4 and 0.050 mol L^{-1} KCl, pH = 2.0. The inset shows the resulting calibration plot. Frequency: 20 Hz; pulse amplitude: 10 mV and step potential: 2 mV.

Flow injection measurements

To speed up the analytical processes, the FIA is an attractive approach as it offers the versatility of operation, high sensitivity, low consumption of samples and reagents, and high analytical throughput compared to batch analysis. To evaluate the CuMEs performance in an FIA system, we used a platform with an array of 20 Cu microsensors and the "wall-jet" flow-cell described in "Flow cell design" sub-section for amperometric detection of glucose. Figure 6A shows the typical I-t curves obtained after injecting 100 μL glucose standard solutions in quadruplicate at 25-600 μmol L^{-1} range concentration in 0.10 mol L^{-1} NaOH used as supporting electrolyte and carrier solution. The amperometric signals exhibited a low background current and excellent reproducibility on the anodic peak current signals for increasing glucose concentration.

At 1.0 mL min^{-1} flow-rate, the method provided an analytical frequency of 80 determinations *per* hour. By using information from the calibration plot in the inset, which followed the equation I (nA) = $1.42 + 0.323 \times C_{glucose}$, μmol L^{-1}, the limit of detection was calculated at 1.7 μmol L^{-1} ($3\sigma_{brank}$). The sensitivity of the 20 CuMEs array was estimated at 734.1 μA $mmol^{-1}$ L cm^{-2} by dividing the slope value of the calibration curve (0.323 nA L μmol^{-1}) by the geometric area of the array (4.40×10^{-4} cm^2). This value is favorable compared to some non-enzymatic methods for glucose sensing reported in the literature,[33-39] and it can be attributed to the highly favorable faradaic-to-capacitive current ratio in the microelectrodes. The high sensitivity confirmed the excellent CuMEs arrays performance for glucose monitoring in low concentrations, like those found in some biological fluids such as salivary and sweat

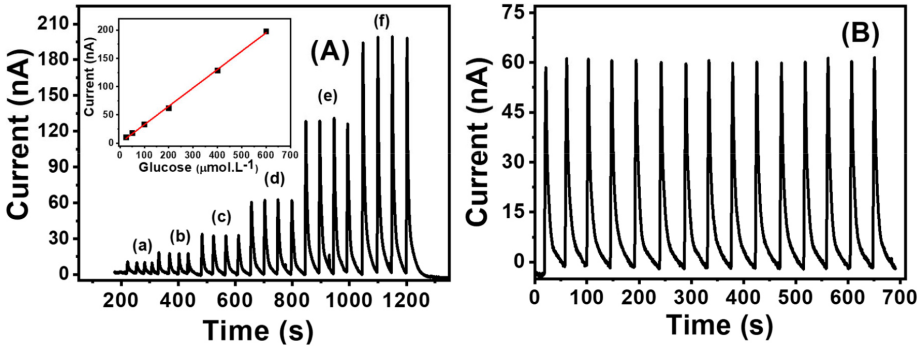

Figure 6. FIA-amperometric signals for increasing glucose concentration on an array of twenty CuMEs in 0.10 mol L^{-1} NaOH carrier solution at 1.0 mL min^{-1} flow rate. Glucose concentration: (a) 25; (b) 50; (c) 100; (d) 200; (e) 400; (f) 600 μmol L^{-1} (A). The inset corresponds to the resulting calibration curve. Repeatability of current signals measured after successive injections of 180 μmol L^{-1} glucose standard solution (B). Working electrode potential: +0.55 V *vs.* Ag/AgCl.

samples. The typical linear concentration range of the method extended from 20 μmol L^{-1} to 4.0 mmol L^{-1}. The glucose reproducibility measurements were evaluated by fifteen 180 μmol L^{-1} glucose solution successive injections in the flow system operating under 1.0 mL min^{-1} flow-rate (Figure 6B). The results indicated a 58.6 nA mean anodic current value and a relative standard deviation (RSD) of 1.70%. The excellent performance demonstrated with the CuMEs array in an FIA system opens new possibilities for sensing applications, including its coupling in electrochemical cells for batch injection analysis (BIA) and liquid-chromatography systems.

Conclusions

Arrays of CuMEs based on microchips have been successfully fabricated. The manufacturing process of copper microelectrodes is simple, cheap, and environmental-friendly. Furthermore, it does not demand either special tools or a highly skilled operator. EDS and cyclic voltammetry were used to investigate the composition of the microelectrodes and the electrochemical behavior in 100 mmol L^{-1} NaOH solution. The CuMEs platforms displayed excellent performance towards the glucose, hydrazine, and nitrate detection in batch and flow cells. By flow injection analysis, the proposed Cu microsensors arrays can detect glucose at a wide dynamic range with high sensitivity (734.1 μA $mmol^{-1}$ L cm^{-2}), demonstrating that they can be a good candidate for glucose monitoring in clinical diagnostics, biotechnology, food industry, and environmental fields.

Supplementary Information

Supplementary data are available free of charge at http://jbcs.sbq.org.br as a PDF file.

Acknowledgments

The authors are grateful to FAPESP (No. 2012/50259-8) for financial support. We also thank MackPesquisa and CNPq for the student grants provided to G.S.H. and G.F.S.

References

1. Martynov, L. Y.; Naumova, O. A.; Zaytsev, N. K.; Lovchinovsky, I. Y.; *Tonkie Khim. Tekhnol.* **2016**, *11*, 26.
2. Pei, X.; Kang, W.; Yue, W.; Bange, A.; Heineman, W. R.; Papautsky, I.; *Anal. Chem.* **2014**, *86*, 4893.
3. Li, Y.; Li, H.; Song, Y.; Lu, H.; Tong, J.; Bian, C.; Sun, J.; Xia, S.; *IEEE Sens. J.* **2016**, *16*, 8807.
4. Paixão, T. R. L. C.; Cardoso, J. L.; Bertotti, M.; *Talanta* **2007**, *71*, 186.
5. Barman, K.; Changmai, B.; Jasimuddin, S.; *Electroanalysis* **2017**, *29*, 2780.
6. Terzi, F.; Zanfrognini, B.; Dossi, N.; Ruggeri, S.; Maccaferri, G.; *Electrochim. Acta* **2016**, *188*, 327.
7. Thi Kim, L. T. O.; Escriou, V.; Griveau, S.; Girard, A.; Griscom, L.; Razan, F.; Bedioui, F.; *Electrochim. Acta* **2014**, *140*, 33.
8. Lin, Y. T.; Chen, C. H.; Lin, M. S.; *Sens. Actuators, B* **2018**, *255*, 2838.
9. Veloso, W. B.; Ribeiro, G. A. C.; da Rocha, C. Q.; Tanaka, A. A.; da Silva, I. S.; Dantas, L. M. F.; *Measurement* **2020**, *155*, 107516.
10. Shukla, R. P.; Belmaker, R. H.; Bersudsky, Y.; Ben-Yoav, H.; *J. Neural Transm.* **2020**, *127*, 291.
11. Wang, Z.; Deng, H.; Chen, L.; Xiao, Y.; Zhao, F.; *Bioresour. Technol.* **2013**, *132*, 387.
12. Rivera, J. F.; Sridharan, S. V.; Nolan, J. K.; Miloro, S. A.; Alam, M. A.; Rickus, J. L.; Janes, D. B.; *Analyst* **2018**, *143*, 4954.
13. Santos, C. S.; Bannitz-Fernandes, R.; Lima, A. S.; Tairum, C. A.; Malavazi, I.; Netto, L. E. S.; Bertotti, M.; *Anal. Chem.* **2018**, *90*, 2587.
14. Gunderson, C.; Zhang, B.; *J. Electroanal. Chem.* **2016**, *781*, 174.
15. Hay, C. E.; Lee, J.; Silvester, D. S.; *Nanomaterials* **2019**, *9*, 1170.
16. da Silva, I. S.; de Araujo, W. R.; Paixão, T. R. L. C.; Angnes, L.; *Sens. Actuators, B* **2013**, *188*, 94.
17. Pacheco, B. D.; Valério, J.; Angnes, L.; Pedrotti, J. J.; *Anal. Chim. Acta* **2011**, *696*, 53.
18. Pedrotti, J. J.; Angnes, L. L.; Gutz, I. G. R.; *Electroanalysis* **1996**, *8*, 673.
19. Orozco, J.; Fernández-Sánchez, C.; Jiménez-Jorquera, C.; *Sensors* **2010**, *10*, 475.
20. Luo, P.; Prabhu, S. V.; Baldwin, R. P.; *Anal. Chem.* **1990**, 752.
21. Dong, S.; Xie, Y.; Cheng, G.; *Electrochim. Acta* **1992**, *37*, 17.
22. He, J. B.; Lu, D. Y.; Jin, G. P.; *Appl. Surf. Sci.* **2006**, *253*, 689.
23. Jiang, L. C.; Zhang, W.-D.; *Biosens. Bioelectron.* **2010**, *25*, 1402.
24. Farrell, S. T.; Breslin, C. B.; *Electrochim. Acta* **2004**, *49*, 4497.
25. Luo, L.; Zhu, L.; Wang, Z.; *Bioelectrochemistry* **2012**, *88*, 156.
26. Ensafi, A. A.; Abarghoui, M. M.; Rezaei, B.; *Electrochim. Acta* **2014**, *123*, 219.
27. Salazar, P.; Rico, V.; González-Elipe, A. R.; *Electroanalysis* **2018**, *30*, 187.
28. Zhang, J.; Zhu, X.; Dong, H.; Zhang, X.; Wang, W.; Chen, Z.; *Electrochim. Acta* **2013**, *105*, 433.
29. Xu, Q.; Zhao, Y.; Xu, J. Z.; Zhu, J. J.; *Sens. Actuators, B* **2006**, *114*, 379.
30. Salazar, P.; Rico, V.; Rodríguez-Amaro, R.; Espinós, J. P.; González-Elipe, A. R.; *Electrochim. Acta* **2015**, *169*, 195.

31. Pletcher, D.; Poorabedi, Z.; *Electrochim. Acta* **1979**, *24*, 1253.
32. Leal, T. F. M.; Fontenele, A. P. G.; Pedrotti, J. J.; Fornaro, A.; *Quim. Nova* **2004**, *27*, 855.
33. Reitz, E.; Jia, W.; Gentile, M.; Wang, Y.; Lei, Y.; *Electroanalysis* **2008**, *20*, 2482.
34. Tang, Y.; Liu, Q.; Jiang, Z.; Yang, X.; Wei, M.; Zhang, M.; *Sens. Actuators, B* **2017**, *251*, 1096.
35. Yang, J.; Tan, W.; Chen, C.; Tao, Y.; Qin, Y.; Kong, Y.; *Mater. Sci. Eng., C* **2017**, *78*, 210.
36. Figiela, M.; Wysokowski, M.; Galinski, M.; Jesionowski, T.; Stepniak, I.; *Sens. Actuators, B* **2018**, *272*, 296.
37. Song, J.; Xu, L.; Zhou, C.; Xing, R.; Dai, Q.; Liu, D.; Song, H.; *ACS Appl. Mater. Interfaces* **2013**, *5*, 12928.
38. Jang, K. B.; Park, K. R.; Kim, K. M.; Hyun, S. K.; Jeon, J. E.; Song, Y. S.; Park, S. K.; Moon, K.-i.; Ahn, C.; Lim, S. C.; Lee, J.; Kim, J. C.; Han, H.; Mhin, S.; *Nanomaterials* **2021**, *11*, 55.
39. Martins, P. R.; Rocha, M. A.; Angnes, L.; Toma, H. E.; Araki, K.; *Electroanalysis* **2011**, *23*, 2541.

Submitted: May 14, 2021
Published online: August 6, 2021